NT-87-07-2



# INFLUENCE OF NATURAL INFILTRATION ON TOTAL BUILDING VENTILATION DOMINATED BY STRONG FAN EXHAUST



**D.E. Kiel, P.E.** **D.J. Wilson, P.E., Ph.D.**
*ASHRAE Member*


ABSTRACT

Tracer gas measurements of the total ventilation rate were made in an unoccupied test house in which an exhaust fan was cycled on and off for four-hour intervals. The exhaust was operated at a flow rate equivalent to 0.85 air changes per hour, and the house leakage configuration - varied by window opening and flue blocking to produce natural infiltration rates - was from 0.1 to 0.5 air changes per hour. Several simple theoretical models for combining fan and natural ventilation flows were compared to the measured data. Direct linear addition of the exhaust and natural flow rates was found to give a superior estimate of the total flow compared to other formulations, including the quadrature superposition recommended in ASHRAE Fundamentals (ASHRAE 1985).

## INTRODUCTION

In order to provide adequate ventilation to maintain indoor air quality, continuous ventilation with an exhaust fan or a balanced flow air-to-air heat exchanger may be necessary. At current energy prices, an exhaust fan is often the most attractive choice because of its low capital and maintenance costs. To avoid oversizing the exhaust fan and causing excessive energy loads, a simple method is required to combine the natural ventilation rate, $Q_{nat}$, with the exhaust fan rate, $Q_{fan}$, to estimate total rate. Because the prediction of natural ventilation rates from infiltration has an uncertainty of about $\pm$ 20% at best, and as much as 50% to 100% if the building leakage sites are not well known, the method for combining this natural infiltration rate with the fan exhaust rate need not have a high level of accuracy, but it should be physically realistic.

Our study will present results for strong exhaust ventilation flows to show that the total ventilation is not well predicted by current models used to combine mechanical and natural flow rates. An improved model will be developed, which accounts for the variation of the fraction of total leakage area participating in infiltration with the strength of the exhaust fan flow rate.

## MODELS FOR COMBINING VENTILATION RATES

The major difficulty in developing a simple theoretical model for superposing natural and mechanical ventilation lies in the nonlinear interaction between the pressures that drive the two flows. For example, mechanical exhaust will depressurize the building and raise the height of the neutral pressure level further above the floor, changing the wind and stack induced natural ventilation flows. Simple models for the combined effect of mechanical and natural ventilation, such as Sherman and Modera's (1984) quadrature superposition, which is used in Chapter 22 of ASHRAE Fundamentals, make the implicit assumption that the effective pressure differences, $\Delta P_{fan}$ for mechanical ventilation and $\Delta P_{nat}$ for natural ventilation, may be added linearly to estimate the net predicted difference, $\Delta P_{pred}$.

$$\Delta P_{pred} = \Delta P_{fan} + \Delta P_{nat} \qquad (1)$$

---

D.E. Kiel and D.J. Wilson, Department of Mechanical Engineering, University of Alberta, Edmonton, Alberta T6G 2G8

which also implies that the effect of wind- and-stack induced flow can be represented by a single effective pressure difference that is unaffected by fan-induced flows. The linear addition of the two pressure differences is correct for local pressures at a given leakage site. However, characterizing the leakage of the sites on an entire building by a single characteristic pressure difference is only a rough approximation. While this single $\Delta P$ assumption is typical of most simple infiltration models, e.g., ASHRAE's (1985), the use of this whole-house $\Delta P$ may not accurately characterize the way in which fan-induced and natural ventilation pressure fields interact. Some caution must be used in drawing physical conclusions from the superposition models developed here from these single characteristic $\Delta P$'s.

The simplest relationship between pressure and flow is Sherman's (1980) orifice flow approximation. The infiltration rate is

$$Q_{inf} = f \frac{A_L}{V} \left( \frac{2\Delta P}{\rho_o} \right)^{0.5} \tag{2}$$

where $A_L$ is the total leakage area (assuming an orifice coefficient of unity) measured by standard fan depressurization methods, and f is the fraction of $A_L$ that is engaged in infiltration. The flow rate is normalized with the interior volume, V, to express Q in air changes per unit time, and the density $\rho_o$ is evaluated at the outdoor temperature. The exfiltration rate is then

$$Q_{exf} = (1-f) \frac{A_L}{V} \left( \frac{2\Delta P}{\rho_i} \right)^{0.5} \tag{3}$$

where (1-f) $A_L$ is the leakage area engaged in exfiltration, and $\rho_i$ is the indoor air density. Considering the level of sophistication inherent in approximating the leakage characteristic as an orifice flow, we will neglect density differences in the following analysis and simply assume $\rho_o = \rho_i = \rho$.

Constant Infiltration Leakage Fraction

The natural ventilation rate is the infiltration in the absence of mechanical ventilation, in which case $Q_{inf} = Q_{exf}$ and $f = 0.5$, so that

$$Q_{nat} = 0.5 \frac{A_L}{V} \left( \frac{2\ \Delta P_{nat}}{\rho} \right)^{0.5} \tag{4}$$

For very weak mechanical ventilation, $Q_{fan}$ is much less than $Q_{nat}$, and the leakage area engaged in infiltration remains constant at $f = 0.5$ with the fan on. The equation for $Q_{fan}$ with $f = 0.5$ is identical to Equation 4 with $\Delta P_{nat}$ replaced by $\Delta P_{fan}$ as the effective pressure. Solving the fan, natural, and total predicted pressures differences allows the linear superposition in Equation 1 to be written in terms of flow rate as

$$Q_{pred} = \left[ Q_{fan}^2 + Q_{nat}^2 \right]^{0.5} \tag{5}$$

for very weak mechanical ventilation. We use the notation $Q_{pred}$ to indicate the total combined flow rate predicted by a model in order to distinguish it from the actual measured total rate, $Q_{tot}$. Equation 5 is the form recommended by Sherman and Modera (1984) and in ASHRAE Fundamentals.

For the limiting case of very strong exhaust, $Q_{fan}$ is much larger than $Q_{nat}$, and this forces the entire leakage area, $A_L$, to act as infiltration sites in both $Q_{fan}$ and the combined predicted total, $Q_{pred}$. With $f = 1.0$ in these two terms, and $f = 0.5$ in the natural ventilation term, it is easy to show that the superposition of pressures in Equation 1 leads to

$$Q_{pred} = \left[ Q_{fan}^2 + \left[ 2\ Q_{nat} \right]^2 \right]^{0.5} \tag{6}$$

for very strong mechanical ventilation. Comparing Equations 5 and 6, we see that in the case

of very strong exhaust, the natural ventilation contributes four times as much to the combined flow as it does in the weak exhaust case.

Variable Infiltration Leakage Fraction

A more realistic approach, which accounts for the gradual increase in infiltration area fraction, f, from 0.5 to 1.0 as mechanical ventilation becomes dominant, has been developed by Wilson and Kiel (1987). Because the inflow and outflow through the building envelope must be in balance,

$$Q_{inf} = Q_{exf} + Q_{fan} \tag{7}$$

Using Equations 2 and 3 in Equation 7, the fraction of leakage area active in infiltration for the combined flow $Q_{pred}$ is

$$f = \frac{1}{\left(2 - \frac{Q_{fan}}{Q_{inf}}\right)} \tag{8}$$

From Equation 7 it is apparent that $Q_{inf}$ is always greater than $Q_{fan}$, so that f must lie in the range $0.5 \leq f \leq 1.0$. If mechanical ventilation acts alone, with no natural ventilation, we have $Q_{inf} = Q_{fan}$ and $Q_{exf} = 0$ in Equation 7. Equation 8 gives $f = 1.0$ because all leakage sites are infiltrating. Equation 2 becomes

$$Q_{fan} = \frac{A_L}{V}\left(\frac{2\Delta P_{fan}}{\rho}\right)^{0.5} \tag{9}$$

The combined mechanical and natural rates are found by using Equation 8 in Equation 2 with $Q_{inf} = Q_{pred}$ to yield the predicted total ventilation

$$Q_{pred} = \frac{1}{V\left(2 - \frac{Q_{fan}}{Q_{inf}}\right)}\left(\frac{2\Delta P_{pred}}{\rho}\right)^{0.5} \tag{10}$$

Solving for the characteristic pressures $\Delta P_{nat}$, $\Delta P_{fan}$, and their sum, $\Delta P_{pred}$ from Equations 4, 9, and 10, and then using the linear superposition of pressures from Equation 1, the resulting flow rate is,

$$Q_{pred} = \left(\left(\frac{Q_{fan}}{2}\right)^2 + Q_{nat}^2\right)^{0.5} + \frac{Q_{fan}}{2} \tag{11}$$

Comparing this to Equation 6 shows that the effect of allowing the infiltration leakage fraction, f, to depend on the strength of mechanical exhaust causes half the exhaust flow to add linearly rather than in quadrature. This tendency for part of the exhaust flow to add linearly to $Q_{nat}$, rather than in a sum of squares, will be significant in interpreting our experimental data.

Other Superposition Models

The most obvious objection to the quadrature superposition, Equation 5, is its implicit assumption of orifice flow. The leakage characteristic of buildings is often better correlated by

$$Q_{inf} = f\frac{C}{V}(\Delta P)^n \tag{12}$$

where C is a constant, and the exponent $n \approx 0.65$ rather than the orifice flow limit of $n = 0.5$. Using Equation 12, the key assumption of linear pressure superposition in Equation 1 leads to

$$Q_{pred} = \left[ Q_{fan}^{1/n} + Q_{nat}^{1/n} \right]^{n} \quad (13)$$

Shaw (1985) used experimental data from infiltration measurements with several types of mechanical ventilation systems to develop superposition models. He defined the boundary between strong and weak mechanical exhaust as the point where the stack-induced flow, $Q_{stack}$, was equal to the forced exhaust rate, $Q_{fan}$, and suggested that the effect of strong mechanical ventilation is to suppress the stack-induced flow, leaving only the wind-induced flow, $Q_{wind}$, to contribute to the total. With this condition, Shaw's superposition model is

$$Q_{pred} = F \left[ Q_{fan}^{1/n} + Q_{wind}^{1/n} \right]^{n} \quad (14)$$

for strong exhaust with $Q_{fan} > Q_{stack}$. The factor F is an empirical correction, which varies from 0.8 to 1.0, to account for the overprediction of total flow by the linear superposition of pressures assumed in Equation 1. Sherman and Modera (1984) and Modera and Peterson (1985) using both experimental data and theoretical calculations have also observed this tendency of the linear pressure superposition of Equations 1 and 5 to overpredict the total flow from combining wind and stack effects.

Levins (1982) suggests a purely empirical model for superposition of a strong exhaust flow on natural infiltration, using data from a clothes dryer exhaust in a single-story house. His nonlinear flow rate superposition is an exponential of the form

$$Q_{pred} = Q_{nat} + Q_{fan} \exp \left[ - \frac{Q_{nat}}{Q_{fan}} \right] \quad (15)$$

In practice, Equation 15 gives almost the same result predicted by the quadrature superposition of Sherman and Modera in Equation 5. At most, Levin's equation predicts a total flow 5% smaller than the quadrature superposition when $Q_{fan} \approx 0.5\ Q_{nat}$ 3% smaller when $Q_{fan} = Q_{nat}$, and only 1% smaller when $Q_{fan} \approx 2\ Q_{nat}$.

## TEST FACILITY

The home heating research facility consists of six unoccupied test houses that have been continuously monitored since 1981 for building envelope energy losses and air infiltration rates. The test houses are located on an agriculture research farm about 10 km south of the city of Edmonton at 53.5°N latitude. They are situated in a closely spaced east-west line with about 2.8 m separation between their side walls. False end walls, with a height of 3.0 m but without roof gable peaks, were constructed beside the end houses of the line to provide equivalent wind shelter and solar shading. The flat exposed site is surrounded by rural farmland, whose fields are planted in forage and cereal crops in summer, becoming snow-covered stubble in winter. Windbreaks of deciduous trees cross the landscape at intervals of a few kilometers, with one such windbreak located about 250 m to the north of the line of houses. The houses are totally exposed to south and east winds. Several single-story farm buildings, located about 50 m to 100 m to the west, provide some shelter from west to northwest winds.

Micrometeorological towers are located midway along the row of houses on both the north and south sides of the house line. The wind speed and direction at a 10 m height are measured with low friction cup anemometers and vanes on both towers, with the data acquisition system recording the value from the tower upwind of the houses. In practice, there was very little difference between upwind and downwind values and the two-tower system simply provided additional reliability. Because the anemometers are located beside the houses they have the same wind exposure but at a height of 10 m, which may be easily corrected to the value at the wall height of 3 m. This means that it is not necessary to account explicitly for terrain roughness and wind shelter from nearby buildings and trees in data correlations.

The present study was conducted on Test House 2, located with one house on its east side and four houses on the west. All houses have identical exterior dimensions and door locations, but with varying types and sizes of windows and air-vapor barriers, and different amounts of thermal insulation. Figure 1 shows the configuration of Test House 2, which is a wood frame bungalow with a 2.6 m deep poured concrete basement and a 46 $m^2$ inside floor area.

about half the area of a typical Canadian single story house. The exterior walls are covered in stained plywood panels over 5 cm of styrofoam insulation. The 2 x 4 stud wall frames are insulated with glass fiber batts, and the interior walls and ceiling are painted drywall over a 0.1 mm (4 mil) polythylene air vapor barrier. The air vapor barrier is penetrated by eight electrical outlet boxes on the inside walls and three light fixture boxes in the ceiling. The air leakage envelope area is 175 $m^2$, including the 5.6 $m^2$ of window area. The heated air volume, including the basement, is 220 $m^3$.

An electric heater is located in the basement with a centrifugal fan distributing air to a single upper room. To promote mixing, there are no permanent interior walls in the house, and the fan operates continuously, recirculating 4.5 air exchanges per hour. The air from the heater vents returns to the basement through a large open stairwell and is picked up by fan intakes at basement floor and ceiling level to avoid stratification. A standard room thermostat controls the interior temperature to about 22°C ± 0.5°C.

Five of the six units, including the one discussed in the present study, have a standard 0.15 m I.D. natural gas furnace flue pipe that acts as the major exfiltration site. This unheated flue begins about 1.5 m above the basement floor and passes through the roof to terminate in a rain cap above the roof ridge. Because the unheated flue is continuously filled with room-temperature air, it is equivalent to a leakage site with the same flow resistance located at a height above the ceiling equal to the distance from the ceiling to the rain cap. Wilson and Dale (1985) found that there was no effect of wind shelter from adjacent houses and nearby buildings on natural air infiltration rates, probably because of the presence of this flue.

Leakage Configurations

The leakage configuration of Test House 2 was altered by opening and closing the sliding window on the west side of the house to create an opening of 214 $cm^2$ and by blocking and unblocking the 177 $cm^2$ area of the 0.15 m diameter chimney flue pipe. House leakage characteristics were determined by mounting a variable-speed fan and a flowmeter in a panel sealed over the opened east-side window and measuring the flow rate over a 2 Pa to 70 Pa range. These data were fitted to the power law of Equation 10 with f = 1.0 to determine C and n. The leakage area $A_{L4}$ at a reference pressure of 4.0 Pa was determined by equating Equations 2 and 12, and the results are summarized in Table 1. The leakage area for flue and window both open was inferred from the other data by finding a flue leakage area of 91 $cm^2$ by difference and adding this to the measured flue-closed, window-open value of 275 $cm^2$.

Mechanical Ventilation System

A centrifugal fan with a constant speed AC motor exhausted room air through an ASME standard orifice meter. The exhaust pipe was sealed into the same panel over the east window that was used for the fan pressurization leakage tests. The metering orifice was sized to produce a flow rate of 51.7 L/s (186 $m^3/h$), which is an air change rate of $Q_{fan} = 0.85\ h^{-1}$. Because the pressure drop through the fan and orifice system was about 180 Pa, of which about 120 was across the orifice, the mechanical ventilation rate was constant and independent of the weather-induced pressures, which were never more than about 10 Pa.

The exhaust fan was operated in an eight-hour cycle, four hours on and four hours off. When the fan was turned off, a motorized low-leakage damper sealed the mechanical exhaust duct. Because the exhaust system was sealed when the fan was off and had a very large pressure drop when the fan was operating, the exhaust system leakage area made no significant contribution to the total leakage area for natural exfiltration. This type of exhaust provides a reasonable simulation of high pressure exhausts with backdraft dampers, but it would be a poor simulation of a low pressure propellor exhaust fan.

Infiltration Measurements

Infiltration measurements were carried out continuously in the six test houses using a constant concentration $SF_6$ tracer gas injection system in each house. Two independent infrared analyzers sampled three houses in sequence through a manifold controlled by solenoid valves, as described in Wilson and Dale (1985).

A microcomputer data-acquisition system monitoring the analyzers was used to control the discrete injections of tracer gas required to maintain the concentration at a constant level of 5 ppm. The sampling system monitored each of the houses for 2.5 minutes with a return

period of 7.5 minutes, which allowed ample time for the previous series of injections to mix completely within the house volume and the time required for the infrared analyzer to draw a sample from an adjacent house. By monitoring and reinjecting tracer gas eight times per hour, the tracer concentration was maintained within 0.2 ppm of the normal 5 ppm set point. Each day at 12:00 p.m. (noon), fresh air was drawn from a line outside the building to check the drift of the $SF_6$ detectors. In addition to the daily zero-concentration readings, the detector was calibrated at monthly intervals using a closed-loop system with syringe injections of $SF_6$ mixtures.

Hourly averages of the tracer gas injection rate were recorded along with indoor and outdoor temperature and wind speed and direction. The measured infiltration rates in $m^3/h$ were divided by the total air volume of 220 $m^3$ to determine the total exchange rate, $Q_{tot}$. An error analysis of the injection and concentration-measuring systems predicted that the standard deviation in air infiltration flow rate was the sum of $\pm$ 2.5% and $\pm$ 0.5 $m^3/h$. For the infiltration measurements recorded in Test House 2, this represents about a $\pm$ 4% standard deviation, or $\pm$ 8% to encompass 95% of the data.

## ESTIMATING NATURAL VENTILATION RATES

To determine how the forced exhaust and natural rates combine, it was necessary to estimate the natural ventilation rate, $Q_{nat}$, that would have occurred during the period when the mechanical ventilation system was active. In our tests, this estimate was made by operating the exhaust fan in four-hour on-off periods, as shown in Figures 2 and 3. Each of these periods produced four hourly averaged ventilation rates from the tracer gas system. The first hour after the exhaust fan was turned on and the first hour after it was turned off tended to produce unreliable data, as the tracer gas system tried unsuccessfully to follow the sudden large change in total ventilation rate. Discarding these hours, the fan-off periods preceeding and following the fan-on period were used to estimate the natural (fan-off) ventilation that would have occurred during the fan-on interval.

To account for weather-induced variations in the natural ventilation rate, the six hourly averages of $Q_{nat}$, U, and $\Delta T$ in the preceeding and following fan-off periods were used to find a least-squares best fit to the current wind and stack "constants", $B_w$ and $B_s$, in the quadrature superposition from ASHRAE (1985).

$$\frac{Q_{nat}^2}{\Delta T} = B_s + B_w \frac{U^2}{\Delta T} \tag{16}$$

The wind speed, U, and temperature difference, $\Delta T$, for each of the last three hours of the fan-on period were then used in Equation 14 to estimate the natural ventilation rate during each hour of the fan-on period. Finally, the estimated natural and measured total values were averaged for these three hours to obtain the $Q_{nat}$ and $Q_{tot}$ values used in the superposition correlations.

## RELATIVE EXHAUST FLOW STRENGTH

Before comparing the measured and predicted total ventilation rates, it is helpful to compare the relative strengths of the exhaust and natural ventilation flows to determine the range of conditions over which the comparisons are made. Figure 4 shows that for the three tightest leakage configurations defined in Table 1 (flue blocked-window closed; flue open-window closed; flue blocked-window open), the mechanical exhaust rate was totally dominant, with $Q_{fan}$ producing about 75% to 85% of the total flow. Only in the leakiest configuration (flue open-window open) did the natural ventilation have any significant effect, and even in this case, the exhaust rate was almost always "strong," varying from 45% to 80% of the total.

Because all the models for superposition of natural and forced ventilation assume a linear addition in Equation 1 of the two independent pressure differences, it is interesting to examine the range of $\Delta P_{fan}$ and $\Delta P_{nat}$ covered by the experiments. The pressure across the building envelope induced by the exhaust fan alone was calculated from Equation 9 for all leakage inward (f = 1.0) and is listed in Table 1 for the four house leakage configurations. For the leakage configuration with flue open and the window closed, the natural infiltration rate, $Q_{nat}$, varied from about 0.1 to 0.5 air changes per hour over the test period. Using $A_{L4}$ = 215 $cm^2$, V = 220 $m^2$, f = 0.5, and $\rho$ = 0.92 $kg/m^3$ in Equation 4, the characteristic natural pressure difference ranged over $\Delta P_{nat} \approx$ 0.2 to 4.0 Pa. This range is roughly the same for all four leakage configurations, changing somewhat because the leakage area was distributed in a different way over the building envelope for each leakage configuration.

Taking the ratio of the natural pressures of 0.2 Pa to 4.0 Pa with the fan-induced pressures of 0.93 Pa to 8.1 Pa, yielded a pressure ratio, $\Delta P_{fan}/\Delta P_{nat}$, that varied by a factor of 200, from 0.25 to 40, with a typical value of about 6.0 for the three tightest leakage configurations. From this, we conclude that our results deal only with the case of strong to very strong mechanical exhaust, where fan-induced pressure differences are dominant.

## COMPARING MEASURED AND PREDICTED TOTAL VENTILATION RATES

The predicted ventilation rates from the superposition theories are compared to tracer gas measurements of the total rate, $Q_{tot}$, in Figures 4 through 8, with a summary comparison in Figure 9. Least-squares linear best fits of the predicted to total ratio versus the ratio of fan to total ventilation are plotted on the figures to show the underprediction or over-prediction and give a reference line about which data variability scatter may be estimated. Perfect agreement between theory and measurement would produce a ratio of predicted to total flow of unity. The results in Figures 4 through 8 indicate that the best agreement with the measurements is obtained either with the linear addition of the two flow rates or with the strong exhaust model that converts all the exfiltration sites to infiltration sites when the fan is on.

This result was totally unexpected, and it conflicts with the experimental results of Shaw (1985), who found that the superposition model of Equation 13, shown in Figure 5, should tend to overpredict the total ventilation rate by about 10% to 20% and not underpredict it by 10% to 25% as indicated by our data. The calculations of total ventilation rate made by Modera and Peterson (1985) suggest that the quadrature superposition shown in Figure 6 should accurately predict (within 10%) the total ventilation rate. Our results show that the quadrature superposition, tends to underpredict the total rate by 15% to 30% over the range of exhaust flows tested. Because Levin's empirical Equation 15 is essentially the same as the quadrature superposition, our results also conflict with his experiments.

The trend lines shown on the figures are linear least-squares best fits to the data. It is important to keep in mind that these trend lines are only for comparison and do not represent any physical model. In fact, the location and slope of the trend lines depends on how much data was taken in each leakage configuration. For example, in Figure 7, if more data had been taken with flue open and window closed (triangles) and less data with both flue and window closed (squares), the trend line may have developed an upward rather than downward slope. Figure 7 also shows that for the same ratio of $Q_{fan}/Q_{tot}$, the location of the leakage site, flue (triangles) vs. window (crosses), affects the agreement with the superposition model. This suggests that a wider range of leakage site locations may be needed for a definitive test of superposition models.

The results in Figure 6 are consistent with a direct linear addition of the natural and mechanical flow rates, rather than a quadrature superposition. If we assume that the actual total rate is the linear sum $Q_{tot} = Q_{nat} + Q_{fan}$, it is easy to show that the quadrature superposition of Equation 5, shown in Figure 6, should underpredict the data by 29% when $Q_{fan}/Q_{tot} = 0.5$ and by 17% when $Q_{fan}/Q_{tot} = 0.8$. This result is close to what we observe, with the least squares data trend line, underpredicting by 31% and by 15% for the two ratios.

Shaw's model from Equation 14 gives even larger underprediction errors than the power law model, because Shaw's superposition assumes that the exhaust pressure cancels the stack-induced component of the natural ventilation rate. In most cases, the wind-induced component, $Q_{wind}$, made the dominant contribution to $Q_{nat}$ in our tests, and Equation 14 predicts total flow rates about 10% less than the power law superposition of Equation 13, which itself underpredicts by 5% to 20%.

The strong mechanical ventilation model of Equation 6 is shown in Figure 7. As expected, because the model assumes that all leakage sites are infiltrating when the fan is on, it overpredicts the total ventilation rate as the exhaust fan rate becomes less strong. In addition, the data scatter is much greater for the strong ventilation model of Figure 7 than for the quadrature superposition of Figure 6. However, this higher variability is expected, because all of the data scatter is due to the variability of $Q_{nat}$, which contributes four times as much to the strong ventilation model as it does to the fixed infiltration fraction model. The very strong exhaust model of Equation 6 gives a more accurate prediction than both the quadrature or power law superpositions of Equations 5 and 13.

The variable infiltration area fraction used in Equation 11 predicts that half the fan ventilation adds in quadrature while the other half adds linearly. As expected, Figure 8

shows that this model lies somewhere between the fixed infiltration fraction quadrature superposition of Figure 6 and the linear addition of flow rates in Figure 4. The use of a variable infiltration area fraction in Equation 11 helps to give some theoretical basis for the unexpected result that a direct linear addition of flow rates gives the best estimate of total flow.

The largest average deviation and highest scatter of data from the trend lines occurred for the leakage configuration with the window closed and the flue open. Under these conditions, the furnace flue acted as an infiltration site (backdrafting) part of the time and as an exfiltration site when the stack effect was large. This flow reversal in a leakage site that contributed to more than 40% of the total leakage area may explain the high variability and large deviation of this data set from the general trend.

## CONCLUSIONS

The main conclusion of our study is that the two separate flow rates due to natural ventilation and mechanical exhaust should be added linearly to give the best estimate for a combined total flow. This finding disagrees with the orifice flow quadrature superposition recommended by ASHRAE Fundamentals. However, this quadrature superposition will underestimate the actual combined flow at most by about 30% and so will give a conservative estimate for the total ventilation rate for the purposes of setting indoor air quality ventilation standards.

This conclusion may not apply to all houses, or even to all leakage configurations for a single house. The test house was unusual in that about one-third of the leakage area was concentrated in the open flue, one-third in the open window, and only the remaining third was in small distributed leakage sites (see Table 1). The location of the flue and window on the building may have influenced the way they change from exfiltration to infiltration sites when the exhaust fan is turned on. A better test of the superposition models would be to increase the leakage area by means of a number of small leakage sites distributed over the envelope. On the other hand, many houses have open flues and windows, and for these situations, the linear flow addition seems to be the best choice.

The underprediction of the quadrature superposition model is due partly to its implicit assumption that the fraction of the leakage area active in infiltration is always a constant regardless of the exhaust flow rate. Comparing Figures 6 and 8 shows that this assumption accounts for about half the 30% underprediction of the quadrature superposition. The remaining underprediction may be due in part to the assumption of a simple linear pressure superposition for the two flows and in part to the orifice flow assumption when the actual flow exponent in our study was $n \simeq 0.6$.

Because our results differ significantly from those of other investigators, more measurements are required, particularly for weak mechanical ventilation, before any definitive statement can be made about the relative merits of quadrature superposition versus linear flow addition. These measurements are now being made.

## REFERENCES


ASHRAE. 1985. "Natural ventilation and infiltration." Chapter 22, ASHRAE handbook-1985 Fundamentals.

Levins, W.P. 1982. "Measured effect of forced ventilation on house infiltration rate." Proceedings: DOE Conference, Thermal Performance of the Exterior Envelopes of Buildings, Las Vegas, December, 1982.

Sherman, M.H. 1980. "Air infiltration in buildings." Ph.D. thesis, University of California. Lawrence Berkeley Laboratory Report, LBL-10712.

Sherman, M.H., and Modera, M.P. 1984. "Comparison of measured and predicted infiltration using the LBL infiltration model." Proceedings ASTM Symposium on Measured Air Leakage Performance of Buildings, Philadelphia, April 1984.

Shaw, C.Y. 1985. "Methods for estimating air change rates and sizing mechanical ventilation systems for houses." National Research Council of Canada, Building Research Note BRN 237, October 1985.

Modera, M., and Peterson, F. 1985. "Simplified methods for combining mechanical ventilation and natural infiltration." Lawrence Berkeley Laboratory Report LBL-18955.

Wilson, D.J., and Kiel, D.E. 1987. "Combining air infiltration rates from natural ventilation and mechanical exhaust." Technical Report, Dept. Mechanical Engineering, University of Alberta.

Wilson, D.J., and Dale, J.D. 1985. "Measurement of wind shelter effects on air infiltration." Proceedings of Conference on Thermal Performance of the Exterior Envelopes of Buildings, Clearwater Beach, Florida, Dec 2-5, 1985.

ACKNOWLEDGMENTS

The study was conducted with grants from Canada Energy Mines and Natural Resources and from the Natural Sciences and Engineering Research Council.

TABLE 1.

Leakage Characteristics for Test House #2

| Symbol | Leakage Configuration flue | window | $A_{L4}$ Leakage Area at 4Pa $cm^2$ | n Exponent | $\Delta P_{fan}$ for $Q_{fan} = 0.85\ h^{-1}$ |
|---|---|---|---|---|---|
| ■ | closed | closed | 124 | 0.64 | 8.1 |
| Δ | open | closed | 215 | 0.58 | 2.7 |
| + | closed | open | 275 | 0.59 | 1.6 |
| □ | open | open | 366* | - | 0.9 |

* estimated using $A_{L4} = 91\ cm^2$ for flue

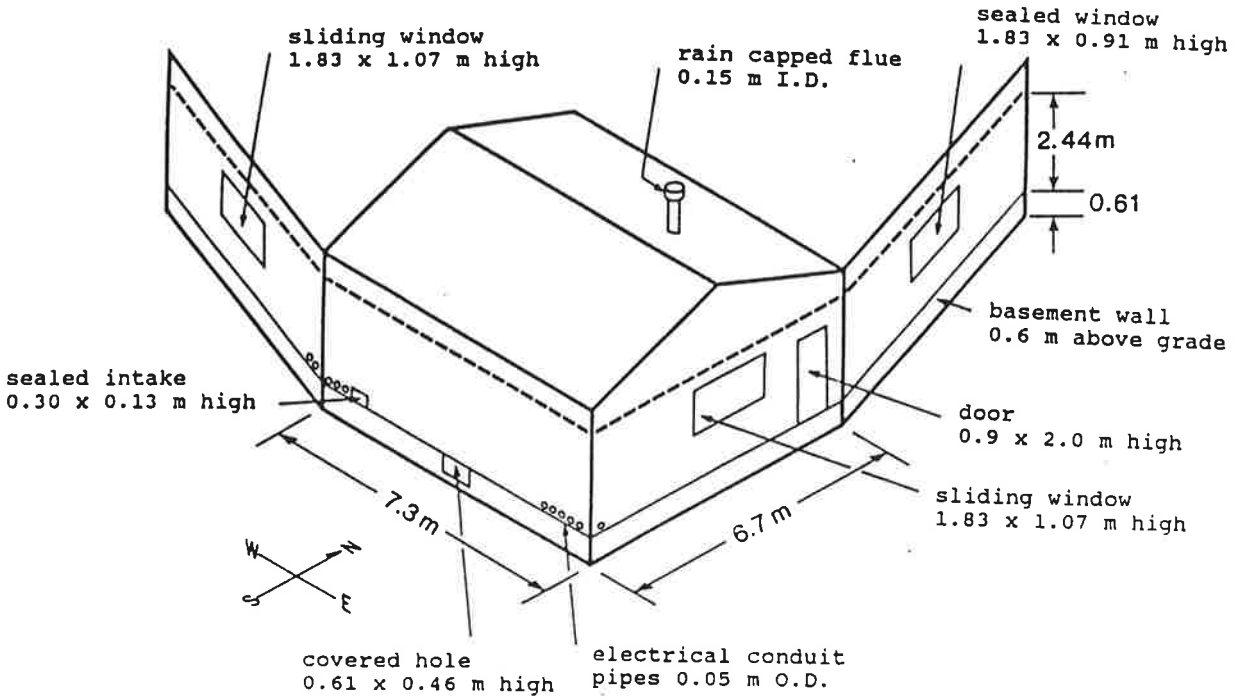


*Figure 1. Infiltration related variables on test house 2 (overhanging roof eaves not shown)*

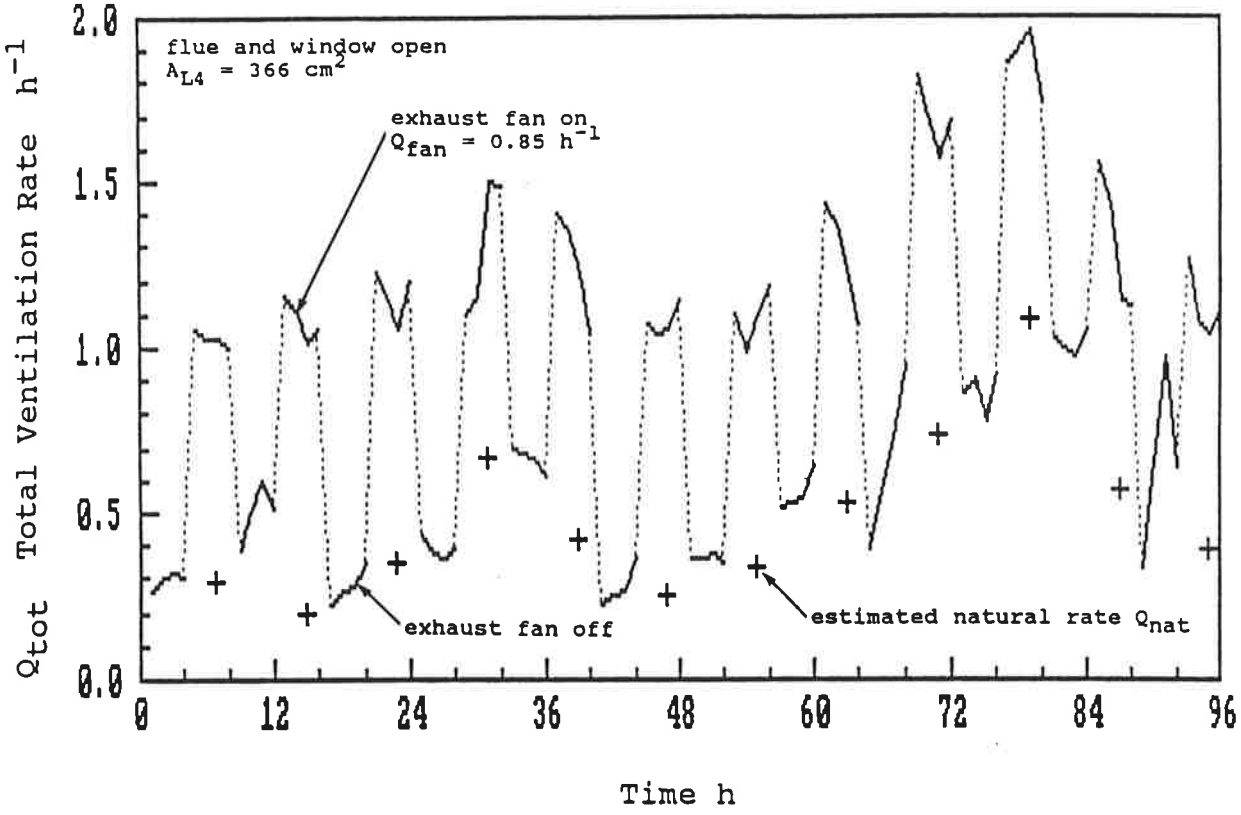


*Figure 2. Typical ventilation rates during exhaust fan cycles for test house 2 in highest leakage configuration*

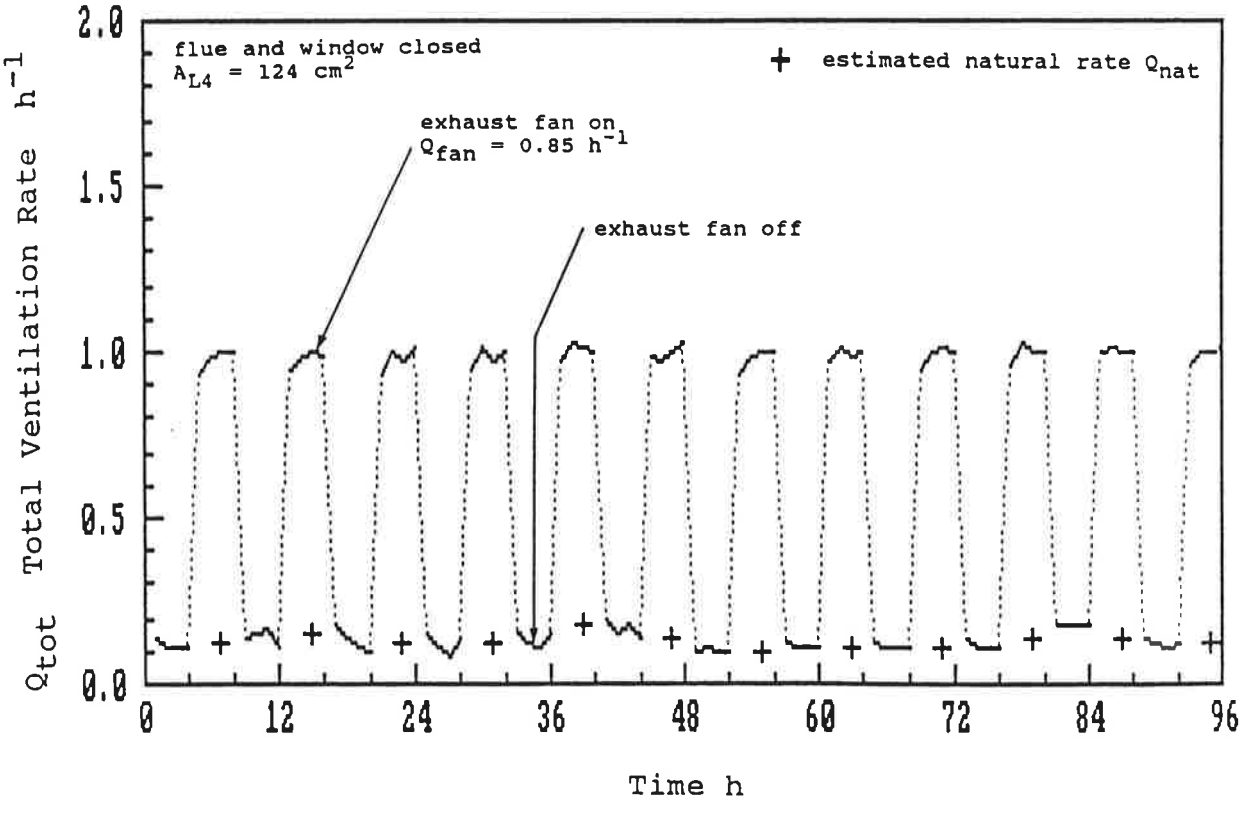


*Figure 3. Typical ventilation rates during exhaust fan cycles for test house 2 in lowest leakage configuration*

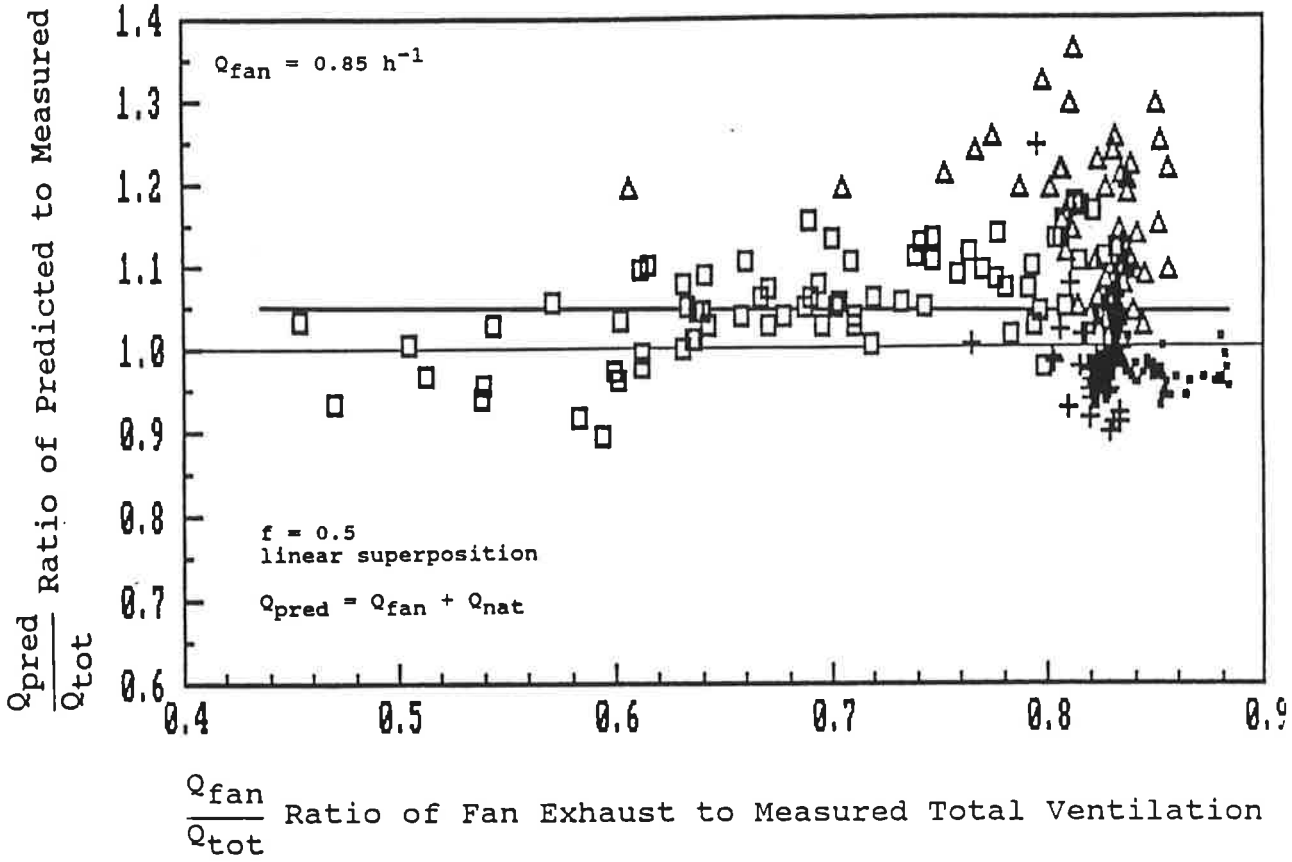


*Figure 4. Linear flow superposition for fixed infiltration area fraction (symbols defined in Table 1)*

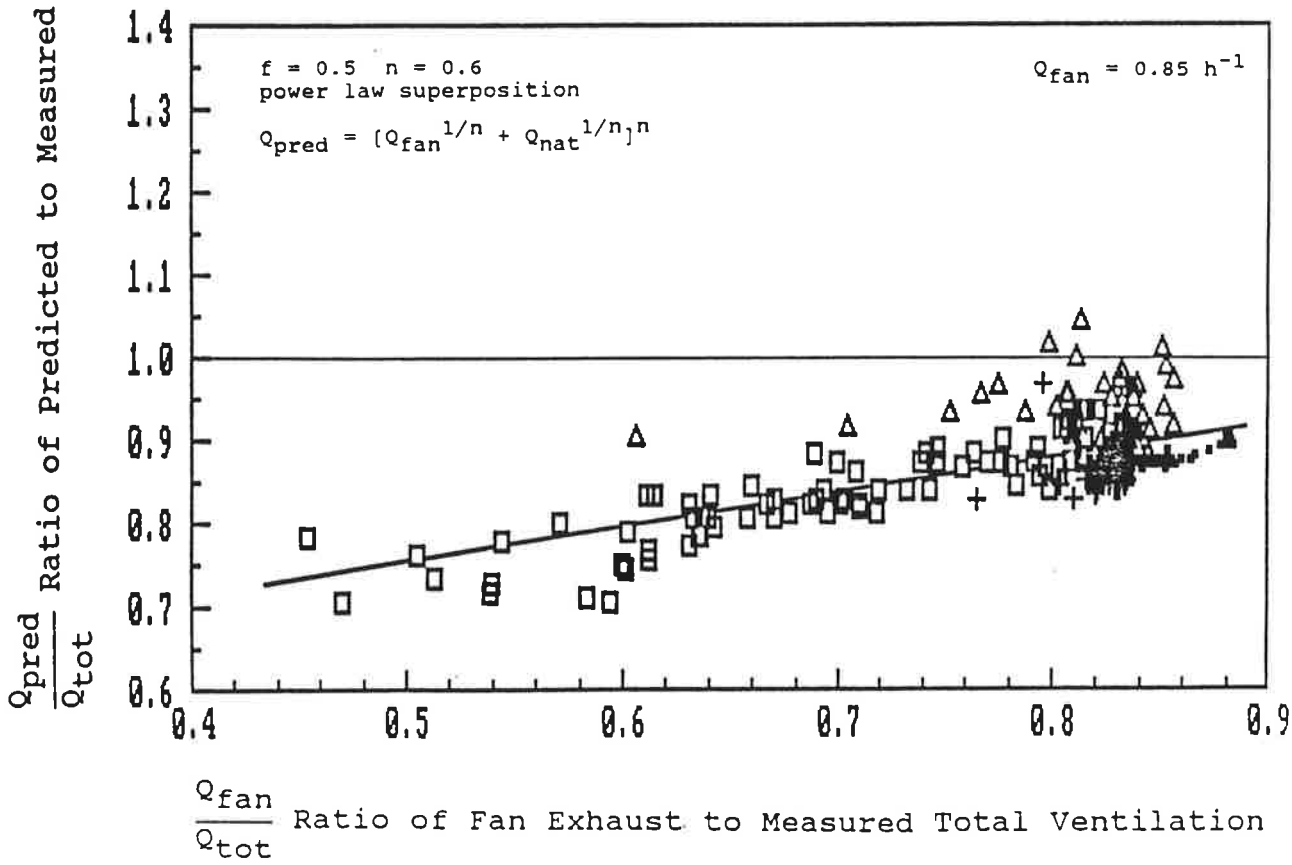


*Figure 5. Power law flow superposition for fixed infiltration area fraction (symbols defined in Table 1)*

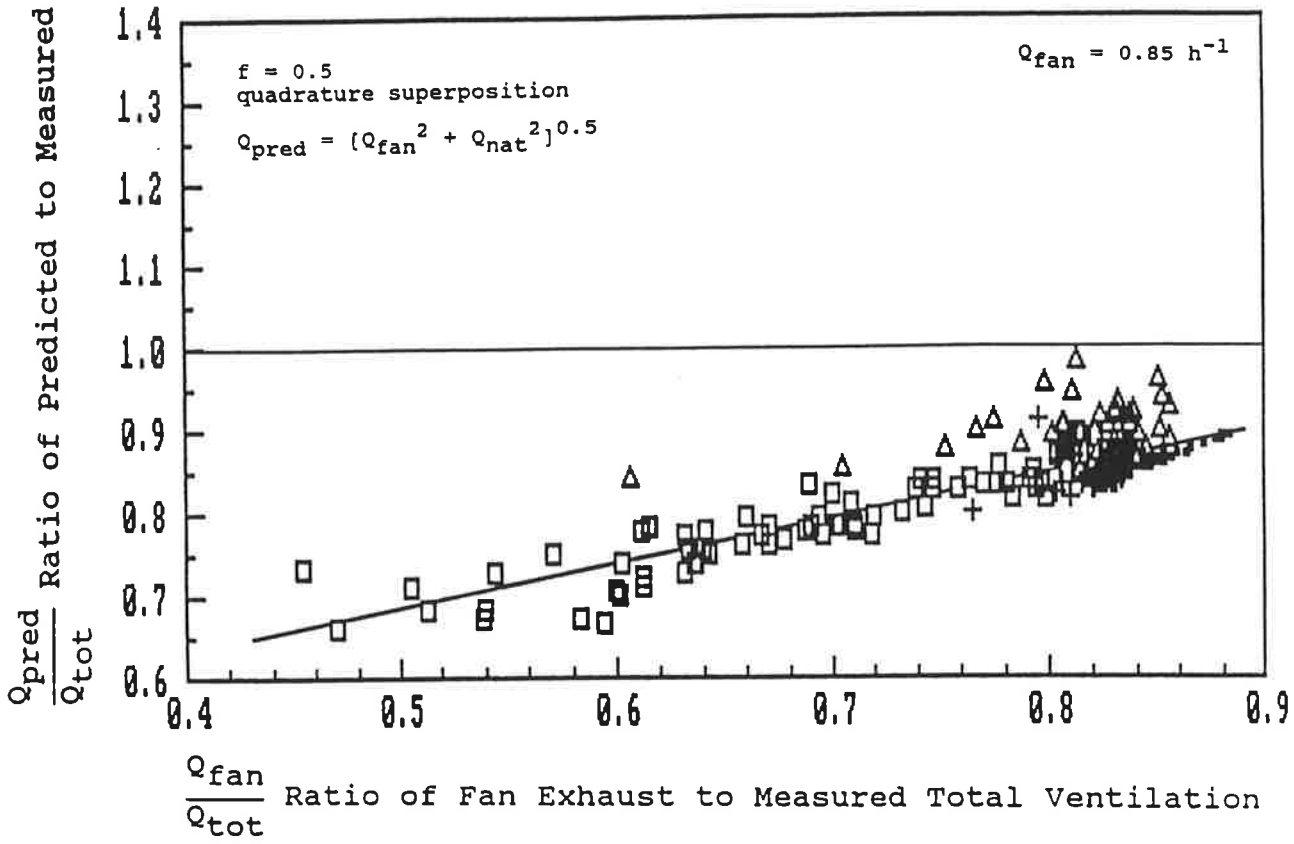


*Figure 6. Quadrature flow superposition for fixed infiltration area fraction (symbols defined in Table 1)*

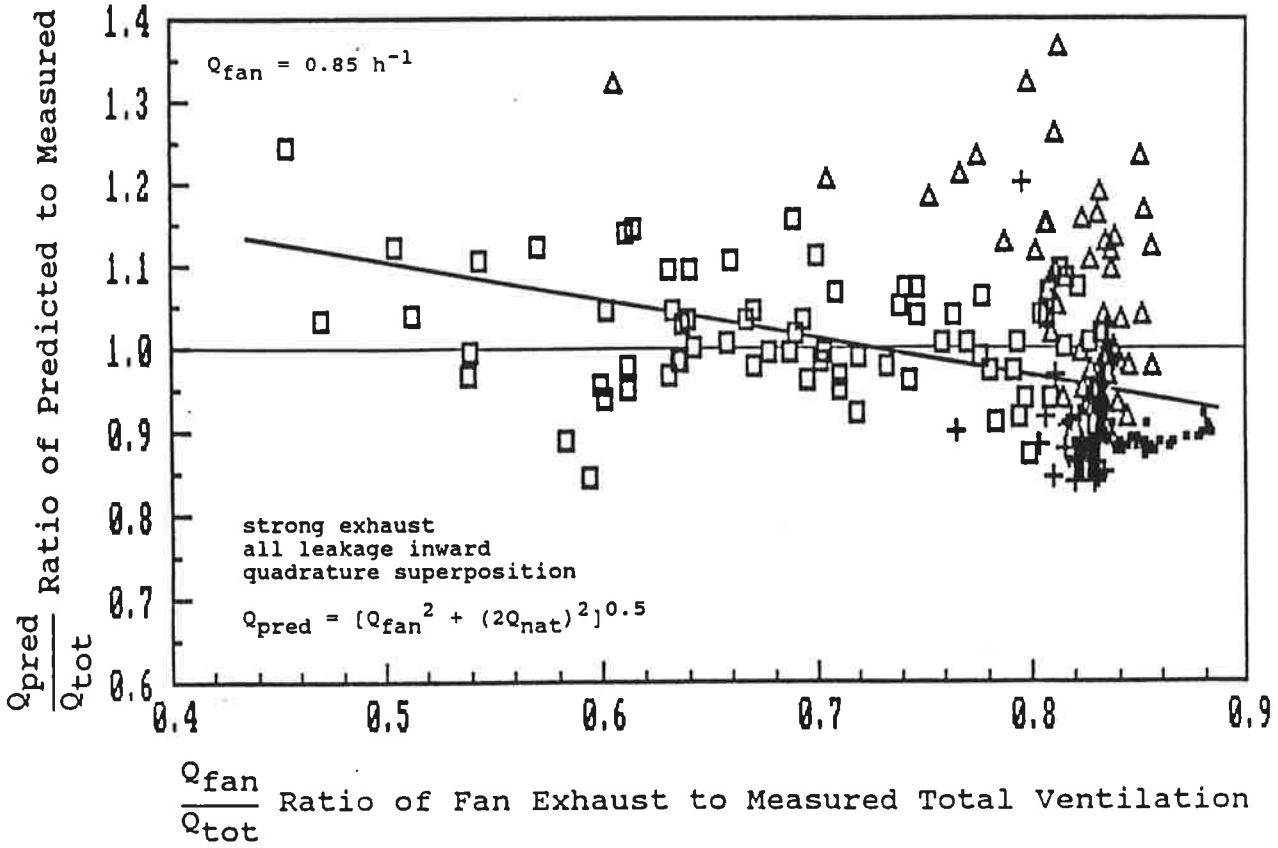


*Figure 7. Quadrature flow superposition for all leakage area infiltrating with strong exhaust and half of leakage area infiltrating with natural ventilation (symbols defined in Table 1)*

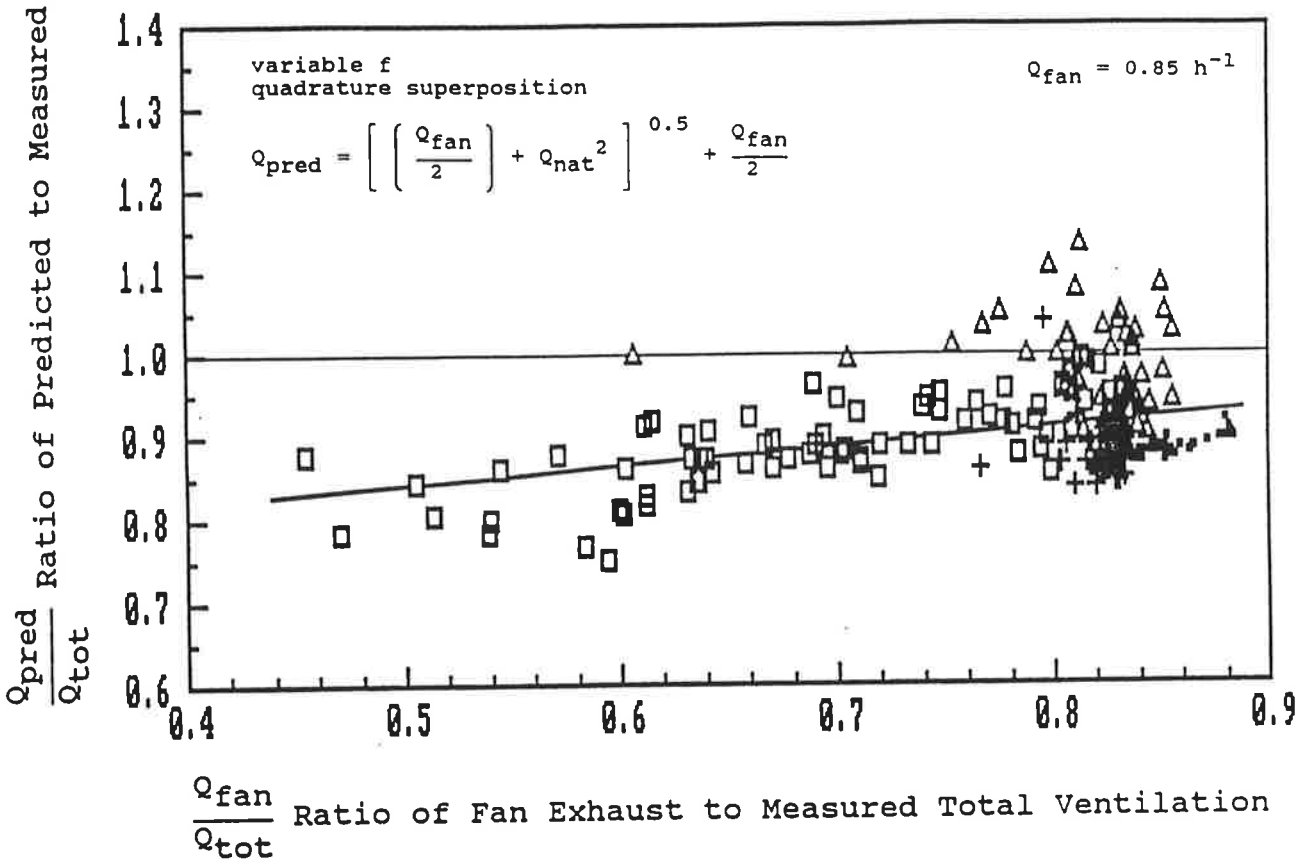


*Figure 8. Quadrature flow superposition for variable leakage area fraction (symbols defined in Table 1)*

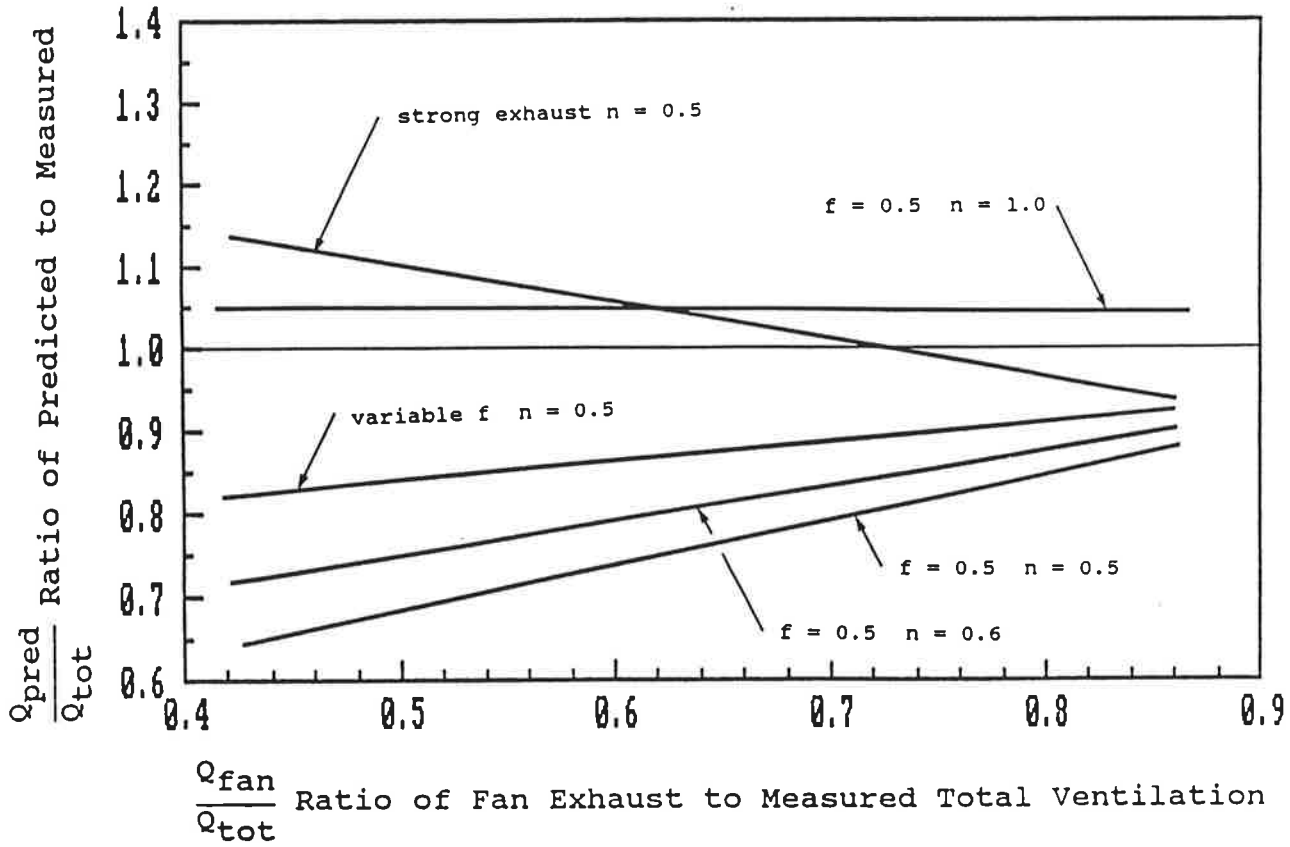


*Figure 9. Summary of data trend correlations for various superposition models (symbols defined in Table 1)*